**Table 4.** Activation Energies of the $Sr_{1+x}Sm_{1-x}FeO_{4-y}$ System as a Function of $x$ Values

| Composition (x) | Activation energy (eV) |
|---|---|
| 0.00 | 0.32 |
| 0.25 | 0.26 |
| 0.50 | 0.17 |
| 0.75 | 0.15 |
| 1.00 | 0.14 |

conductivity increases with temperature. As has been observed in perovskite and $K_2NiF_4$ system, the ratio of $Fe^{4+}$ ion seems to play an important role in conduction mechanism. When very small amount of $Fe^{4+}$ exists or only $Fe^{3+}$ exists in a ferrite, the conductivity is very low. However, the conductivity of ferrite containing considerable amount of $Fe^{4+}$ shows much increased conductivity at constant temperature. In the system, unlike $Sr_{1+x}Dy_{1-x}FeO_{4-y}$ system where the sample of $x=0.00$ had low conductivity, all the samples shows slight change in conductivity with $x$ value. Such a difference can be explained using Table 2. The sample of $x=0.00$ has about 20% of $Fe^{4+}$ ion, and accordingly shows relatively higher conductivity than $Sr_{1.00}Dy_{1.00}FeO_{4.04}$ system.

In $Sr_2FeO_{3+x}F_{1-x}$ system, $Sr_2FeO_{3.20}F_{0.80}$ where $Fe^{4+}$ content was 20% was prepared under 1300 K in air. The study of thermal variation of the conductivity for $Sr_2FeO_{3.20}F_{0.80}$ shows typical semiconductivity, and the activation energy is 0.26 eV. The activation energy value is similar to that of the sample with $x=0.25$ ($Fe^{4+}$ content is 30%) in our system. The activation energy decreases with increase in $x$ value (Table 4).

## References


1. Shimada, M.; Koizumi, M.; Dakano, M.; Shinjo, T.; Takada, T. *J. De Phisique* **1979**, *40*, C2-272.
2. Yo, C. H.; Lee, E. S.; Pyon, W. B.; Pyon, M. S. *J. Kor. Chem. Soc.* **1988**, *32*, 3.
3. Menil, F.; Kinomura, N.; Fournes, L.; Portier, J.; Hagenmuller, P. *Phys. Stat. Sol.* **1981**, *64*, 261.
4. Soubeyroux, J. L.; Courbin, P.; Fournes, L.; Fruchart, D.; LE Flem, G. *J. Solid State Chem.* **1980**, *31*, 313.
5. Puche, R. S.; Norton, M.; Glaunsinger, W. S. *Mat. Res. Bull.* **1982**, *17*, 1429.
6. Demazeau, G.; LI-Ming, Z.; Fournes, L.; Pouchard, M.; Hagenmuller, P. *J. Solid State Chem.* **1988**, *72*, 31.
7. Ganguly, P.; Rao, C. N. R. *Mat. Res. Bull.* **1973**, *8*, 405.
8. Berjoan, R.; Coutures, J. P.; LE Frem, G.; Saux, M. *J. Solid State Chem.* **1982**, *42*, 75.
9. Nguyen-Trut-Dinh, M. M.; Vlasse, M. Perrin, M.; LE Frem, G. *J. Solid State Chem.* **1980**, *32*, 1.
10. LE Frem, G.; Demazeau, G.; Hagenmuller, P. *J. Solid State Chem.* **1982**, *44*, 82.
11. Yo, C. H.; Lee, E. S.; Pyon, M. S. *J. Solid State Chem.* **1988**, *73*, 411.
12. Grenier, J. C.; Pouchard, M. *Mat. Res. Bull.* **1984**, *19*, 1301.
13. Dakano, M.; Kawachi, J.; Nakanishi, N.; Takeda, Y. *J. Solid State Chem.* **1981**, *39*, 75.
14. Gallagher, P. K.; Macchesney, J. B.; Buchanan, D. N. E. *J. Chem. Phys.* **1966**, *45*, 2466.


# Electronic Structure Study of the Formal Oxidation States of Lead and Copper in $Pb_2Sr_2ACu_3O_8$ (A=Ln, Ln+Sr, or Ln+Ca) and Their Possible Changes upon Oxidation

**Dae-Bok Kang**

*Department of Chemistry, Kyungsung University, Pusan 608-736, Korea*

*Received November 17, 1995*

We examined the formal oxidation states of Pb and Cu in the $Pb_2CuO_4$ slab of $Pb_2Sr_2ACu_3O_8$ ($A=Y_{1-x}Ca_x$ or $Nd_{1-x}Sr_x$) and their possible changes by oxygen incorporation in the Cu layer of the slab by performing tight-binding band electronic structure calculations on the $Pb_2CuO_{4+\delta}$ slab. Our results show that the most likely oxidation state of Pb is +2 and that of Cu is +1 for the $Pb_2CuO_4$ slab prior to oxidation. With small $\delta$ values, the oxygen incorporation occurs by the formation of such chain fragments as in $YBa_2Cu_3O_{7-y}$ along the **a**+**b** axis. The four-coordinate Cu atoms in the chain fragments are in the +3 oxidation states. For values of $\delta$ larger than 0.5, however, an additional oxygen ($O_{ad}$) goes to the site along the **b** axis to form short Pb-$O_{ad}$ distances oxidizing $Pb^{2+}$ to $Pb^{4+}$. This change in the Pb oxidation state leads to the suppression of superconductivity due to the decrease of holes in the $CuO_2$ layer.

## Introduction

High-temperature superconductivity ($T_c$~70 K) has been identified in a family of Pb-containing copper oxide materials with formula $Pb_2Sr_2ACu_3O_{8+\delta}$, where A is a mixture of lanthanide (Y, Nd etc) and alkaline earth (Ca or Sr) elements

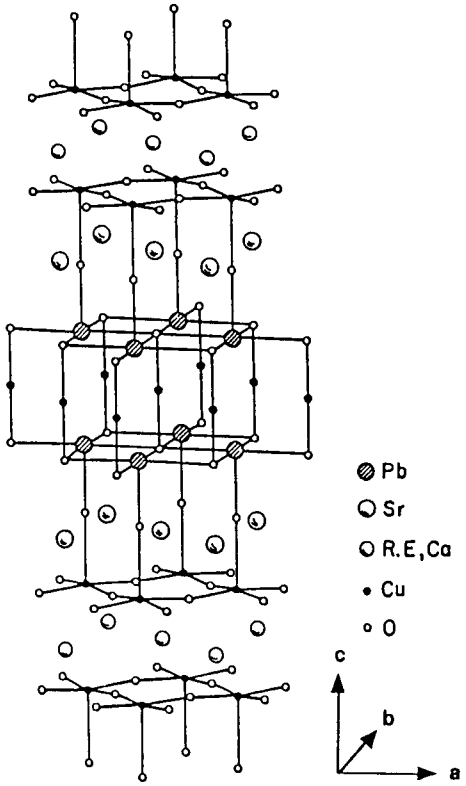


**Figure 1.** Crystal structure of $Pb_2Sr_{2.24}Nd_{0.76}Cu_3O_8$ taken from Reference 1.

and the oxygen content δ is variable over a wide range ($0 \leq \delta \leq 1.8$).[1,2] The structure was refined from X-ray powder diffration data in Cmmm with $\sqrt{2}a_p \times \sqrt{2}a_p \times c$ unit cell ($a_p$ = unit cell edge of the simple perovskite structure) by Cava *et al.*[1] and from X-ray single-crystal data in P4/mmm with an $a_p \times a_p \times c$ unit cell (obtained by rotating 45° around c) by Subramanian *et al.*[2] These refinements give essentially the same arrangements.

The peculiar structural feature of this Pb-containing family is the $Pb_2CuO_4$ slab sandwiched between two $CuO_2$ sheets in each $Pb_2Sr_2Cu_3O_8$ slab as shown in Figure 1. Each $Pb_2CuO_4$ slab is constructed from two rock salt-type Pb-O sheets by joining the equatorial oxygen atoms ($O_{eq}$) with Cu atoms to form "linear" $O_{eq}$-Cu-$O_{eq}$ linkages. Each Pb atom of the Pb-O sheet is capped by an axial oxygen atom ($O_{ax}$), which is shared with a Cu atom of the neighboring perovskite-type $CuO_2$ layer to form linear Pb-$O_{ax}$-Cu linkages. Thus, the $Pb_2CuO_4$ slab consists of square pyramidal five-coordinate Pb and two-coordinate Cu. Given the formal oxidation states +2 and +1 for the Pb and Cu atoms of the $Pb_2CuO_4$ slab, the formal oxidation state of Cu in the $CuO_2$ layer is given by $2+x/2$ for $Pb_2Sr_2(Ln_{1-x}M_x)Cu_3O_8$, where Ln and M refer to lanthanide and alkaline earth elements, respectively. Namely, doping of the Ln positions of the prototype compound $Pb_2Sr_2LnCu_3O_8$ with M atoms creates holes in the $CuO_2$ layers, and thereby inducing the superconductivity.[3]

The $Pb_2Sr_2(Ln_{1-x}M_x)Cu_3O_8$ can be oxidized at low temperature to give $Pb_2Sr_2(Ln_{1-x}M_x)Cu_3O_{8+\delta}$ phases with various values of $0<\delta<2$, some of which exhibit superconductivity at the range of temperatures between 10 and 70 K for the samples with a value of δ less than 1. Thus an interesting relationship exists among $T_c$, δ and M : Ln ratio in $Pb_2Sr_2(Ln_{1-x}M_x)Cu_3O_{8+\delta}$.[4,9] The superconcuctivity in each compound with different $x$ is found to be suppressed with a large δ. In understanding the superconductivity of $Pb_2Sr_2(Ln_{1-x}M_x)Cu_3O_{8+\delta}$, it is crucial to know the formal oxidation states of Pb and Cu atoms in the $Pb_2CuO_4$ slab since they can cause a change of the hole concentration in the $CuO_2$ layer. We note that the chemistry of oxide superconductors cannot be discussed without reference to the concept of formal oxidation states employed for the purpose of counting the number of electrons. As an example, when five Cu 3d-block orbitals (which are antibonding between Cu 3d orbitals and surrounding oxygen 2p orbitals) are occupied by 8, 9, and 10 electrons, the copper oxidation states are $Cu^{3+}$, $Cu^{2+}$, and $Cu^{+}$, respectively. Likewise, when the Pb 6s-block orbital (which is antibonding between Pb 6s and surrounding O 2p orbitals) is occupied by two electrons, the lead oxidation state is $Pb^{2+}$. By definition, the oxidation state of oxygen in the oxide superconductors is $O^{2-}$ if all the oxygen s- and p- block levels are fully occupied.

In the present study, we investigate effects of the additional oxygen sites on the formal oxidation states of Pb and Cu atoms of $Pb_2Sr_2(Ln_{1-x}M_x)Cu_3O_8$ and also of the oxidation on the hole concentration in the $CuO_2$ layer and superconductivity by performing tight-binding band calculations[5] within the framework of the extended Hückel method.[6] The atomic parameters employed in this study are summarized in Table 1.

**Table 1.** Atomic Parameters Used in the Calculations

| atom | orbital | $H_{ii}$, eV | $\zeta_1$[a] | $\zeta_2$[a] | $c_1$[b] | $c_2$[b] |
|---|---|---|---|---|---|---|
| Pb | 6s | −18.70 | 2.57 | | | |
| | 6p | −10.80 | 2.13 | | | |
| Cu | 4s | −11.40 | 2.20 | | | |
| | 4p | −6.06 | 2.20 | | | |
| | 3d | −14.00 | 5.95 | 2.30 | 0.5933 | 0.5744 |
| O | 2s | −32.30 | 2.275 | | | |
| | 2p | −14.80 | 2.275 | | | |

[a] Slater type orbital exponents. [b] Contraction coefficients of a double-ζ expansion.

## Structure of $Pb_2CuO_4$ Slab

With the model (Figure 1) reported by Cava *et al.* the thermal factor of the oxygen atoms in PbO layers is abnormally high, indicating that the oxygen atoms are not fixed to a single position. When the oxygen atoms of the PbO layer (*i.e.*, $O_{eq}$) are all in the "average" positions, the Pb-$O_{eq}$ layer is represented by **1**, which forms rather long Pb-O distances of ~2.7 Å. The structure refined by Subramanian *et al.* is essentially similar to Cava *et al*'s, but the $O_{eq}$ atoms in the PbO layer are represented in **2** by four split positions around the idealized oxygen sites, giving some reasonable Pb-O distances of ~2.4 Å. Given the four split positions for each $O_{eq}$ atom, one can generate several patterns of the PbO layer by selecting one of the four $O_{eq}$ positions. One simple pattern is shown in **3** (Pb-$O_{eq}$ = 2.40 and 3.04 Å). The oxygen-

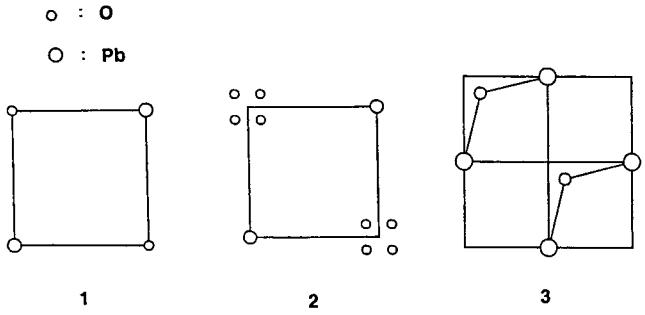


free Cu layer is introduced in between two PbO layers. The Cu atoms have a stick coordination with two $O_{eq}$ atoms. Depending upon which of the two $O_{eq}$ positions are occupied the $O_{eq}$-Cu-$O_{eq}$ angles are either linear or bent. Then the relative arrangements of two such PbO layers in the $Pb_2CuO_4$ slab of $Pb_2Sr_2(Ln_{1-x}M_x)Cu_3O_8$ are depicted in **4a, 4b,** and **4c**, where the solid and the dashed lines refer to the patterns

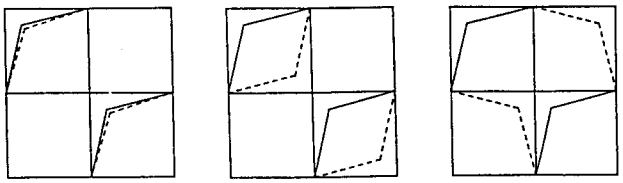


of the upper and the lower PbO layers, respectively. The Cu-$O_{eq}$ bonds in these arrangements **4** are somewhat longer than those in the ideal arrangement **1** (Cu-$O_{eq}$=1.88 Å in **4** and Cu-$O_{eq}$=1.83 Å in **1**). There are many other possible Pb-$O_{eq}$ sheet patterns, but the two examples **1** and **4a** are sufficient for our purpose as will be discussed later.

Previous band electronic structure calculations on $Bi_2Sr_2Ca_{n-1}Cu_nO_{2n+4}$[7] and $Tl_mBa_2Ca_{n-1}Cu_nO_{2n+m+2}$[8] showed that the rock salt layer structures have profound effects on the positions of the rock salt layer bands with respect to the Fermi level and therefore on the hole concentration in the $CuO_2$ layer. Thus it is necessary to consider several model structures of $Pb_2CuO_{4+\delta}$ slab in electronic structure calculations on $Pb_2Sr_2(Ln_{1-x}M_x)Cu_3O_{8+\delta}$. However, band calculations on the isolated $Pb_2CuO_4$ slab structures with and without displacements of oxygen atoms in the PbO layers have given essentially the same results, so that we adopt the latter structure (see **1**) in our calculations.

## Electronic Structure and Discussion

**$Pb_2CuO_4$ Slab.** In $Pb_2Sr_2(Ln_{1-x}M_x)Cu_3O_8$ the highest occupied band (*i.e.*, the $x^2$-$y^2$ band) of the $CuO_2$ perovskite layer is primarily constructed from the $x^2$-$y^2$ orbital of the copper atom and the $p$ orbitals of the in-plane oxygen atoms. The $x^2$-$y^2$ orbital of Cu is of δ symmetry with respect to the Cu-$O_{ax}$-Pb axis, so that the $x^2$-$y^2$ band of the $CuO_2$ layer does not have any orbital contribution from the PbO rock salt layers. Likewise, the Pb bands of the PbO layers have no $x^2$-$y^2$ orbital contribution from the $CuO_2$ layers. We therefore performed band calculations on the isolated $Pb_2CuO_4$ slab to determine the formal oxidation states of lead and copper atoms. The band dispersion relations calculated for the $Pb_2CuO_4$ slab are shown in Figure 2, where the dashed line refers to the Fermi level (−11.75 eV) of the half-filled $x^2$-$y^2$ bands of the $CuO_2$ layers taken from $Pb_2Sr_2(Nd_{0.76}Sr_{0.24})Cu_3O_8$ phase.[1] In Figure 3 we present the density of states (DOS) plots indicating its projected contribution to provide a comprehensive overview of the band electronic structure. It is important to examine whether or not the 6s- and 3d- block bands originating from Pb and Cu lie below the Fermi level. The projected Pb DOS results in Figure 3a reflect the presence of the 6s-block bands below the Fermi level. The structure at higher energies (−10 to −6 eV) contains a predominant 6p character (Figure 3b), which is antibonding in the Pb-O bonds as shown in the crystal orbital overlap population (COOP) curves of Figure 3c. Thus the oxidation state of Pb is expected to be +2 (*i.e.*, its 6s-block bands are occupied, but the 6p-block bands are empty). In Figure 3d the 3d-block bands of the oxygen-free Cu layer do not contribute at all to the DOS above the Fermi level, which suggests that the oxidation state of these copper atoms is +1. The oxidation states of these atoms are consistent with the oxidation states assigned to them in References 1 and 2.

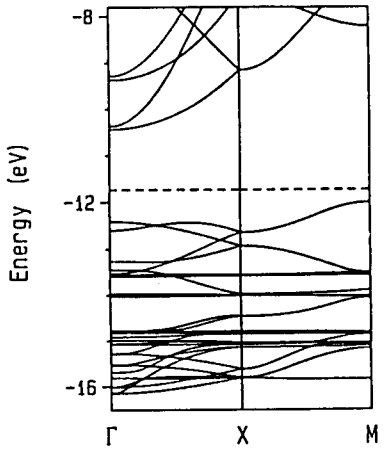


**Figure 2.** Band electronic structures calculated for the $Pb_2CuO_4$ slab. The dashed line refers to the Fermi level of the half-filled $CuO_2$ layer $x^2$-$y^2$ band. In units of the reciprocal vectors $a^*$ and $b^*$, the wave-vector points Γ, $X$, and $M$ are given as follows: Γ=(0, 0), $X$=($a^*$/2, 0), and $M$=($a^*$/2, $b^*$/2).

If we introduce in the calculations the slight displacements of the oxygen atoms in the PbO layer given by **4a**, its distinctive DOS feature (Figures 4a and b) originating from lead 6s- and 6p- and copper 3d-block bands is very similar in shape and position to the corresponding one shown in Figures 3a, b, and d. This striking fact indicates that these bands are not so sensitive to small displacements of the oxygen atoms in the PbO layers, which is why we adopt the ideal structure without oxygen displacement in our study as already mentioned.

**Oxidation of $Pb_2CuO_4$ Slab.** While $Pb_2Sr_2YCu_3O_8$ is an antiferromagnetic semiconductor like $YBa_2Cu_3O_6$, it can be transformed into superconductors by partial substitution of divalent Ca ions for $Y^{3+}$, which results in an oxidation of the $CuO_2$ layers leaving the copper oxidation state of the O-free Cu layers unchanged. This indicates that the holes formed on the Y/Ca layers are doped into the $CuO_2$ layers,

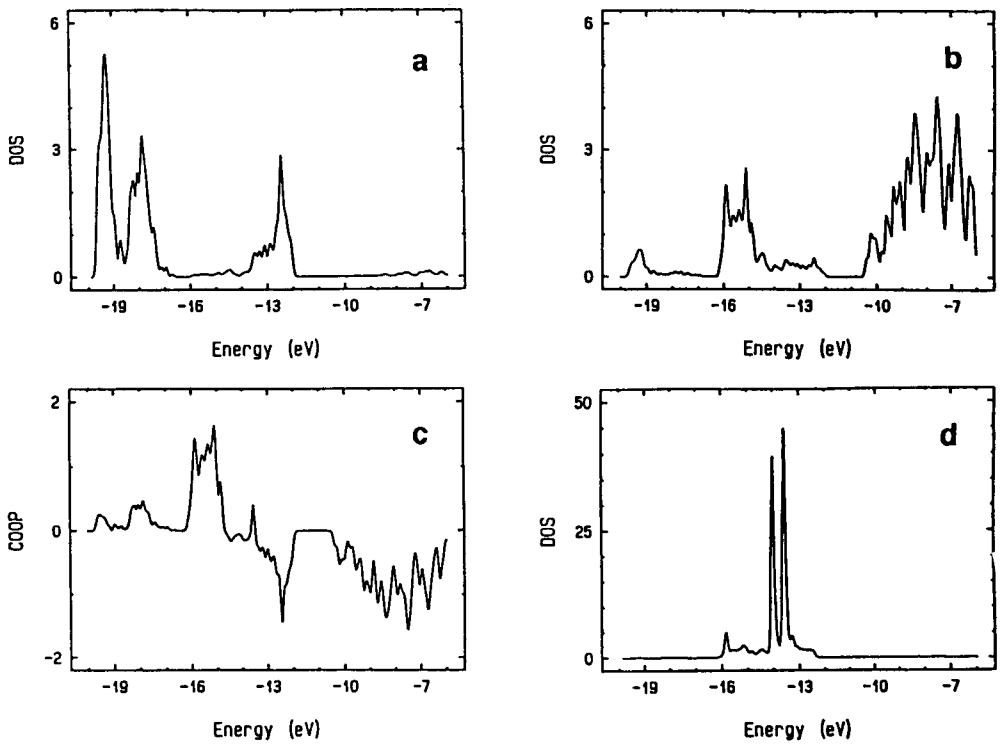


**Figure 3.** Projected DOS plots on Pb 6s (a), Pb 6p (b), and Cu 3d (d); COOP plots for the Pb-O bonds (c) in $Pb_2CuO_4$ slab.

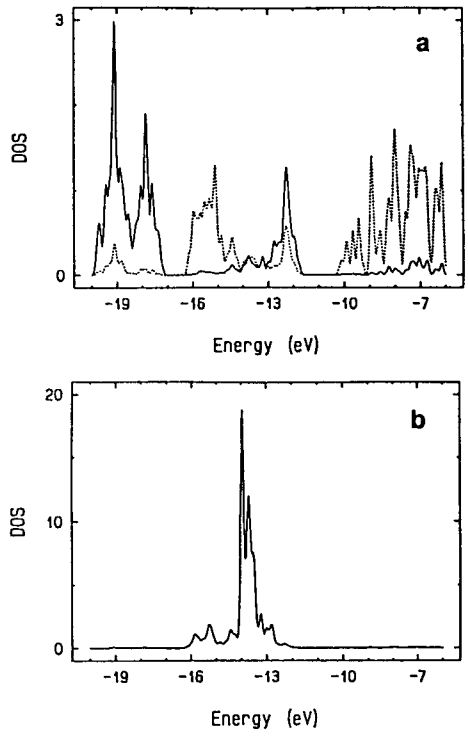


**Figure 4.** Projected DOS plots on Pb 6s (solid line) and Pb 6p (dotted line) (a) and Cu 3d (b) in $Pb_2CuO_4$ slab with the PbO layer given by **4a**.

leading to the appearance of superconductivity as stated in introduction of this paper. It has been found that the superconducting transition temperature ($T_c$) of $Pb_2Sr_2Y_{1-x}Ca_xCu_3O_8$ increases with increasing $x$ and takes a maximum at $x=0.5$.[9] The hole concentration of the $CuO_2$ layers ($n_H$) increases with increasing $x$. According to our empirical relationship between $T_c$ and $n_H$,[3] there exists an optimum hole concentration ($n_{opt}$) for which $T_c$ is maximum so that $T_c$ increases with $n_H$ for $n_H<n_{opt}$ (*i.e.*, underdoped hole region), but decreases with $n_H$ for $n_H>n_{opt}$ (*i.e.*, overdoped hole region). Therefore, an optimum hole concentration for $Pb_2Sr_2Y_{1-x}Ca_xCu_3O_8$ is achieved with $x=0.5$ when the oxidation state of copper atoms in the $CuO_2$ layer becomes +2.25.

The superconducting $Pb_2Sr_2Y_{1-x}Ca_xCu_3O_8$ is readily oxidized since additional oxygens ($O_{ad}$) can be most probably incorporared in the Cu layer sandwiched between two PbO layers having enough space to make available such an incorporation. In $Pb_2Sr_2Y_{1-x}Ca_xCu_3O_{8+\delta}$ the superconductivity appears to depend on which additional oxygen site is occupied for $\delta>0$. To clarify the role of the Pb and Cu oxidation states upon oxidation in superconductivity, therefore, we examine the oxidation process of the compound by considering the oxidation/reduction potentials of the $Pb^{4+}/Pb^{2+}$ and the $Cu^{2+}/Cu^{+}$ systems and the experimental results[4] of dependence on $\delta$ of the lattice constants, the average oxidation states of Pb and Cu, the hole concentration, and the resistivity *vs.* temperature correlation. The redox potential of $Cu^{2+}/Cu^{+}$ is smaller than that of $Pb^{4+}/Pb^{2+}$ and so the oxidation of the Cu cations should take place prior to that of the Pb ones. This fact implies that at the beginning of the oxidation process the oxygen atoms are incorporated into the Cu layers to form the same Cu-O corner-sharing square chains as in $YBa_2Cu_3O_{7-y}$ that would formally oxidize $Cu^{+}$ to $Cu^{3+}$. However, after a small amount of oxygen incorporation this process is completed and then the further incorporation of oxygen takes place at other sites on the $CuO_8$ plane *i.e.*, at the

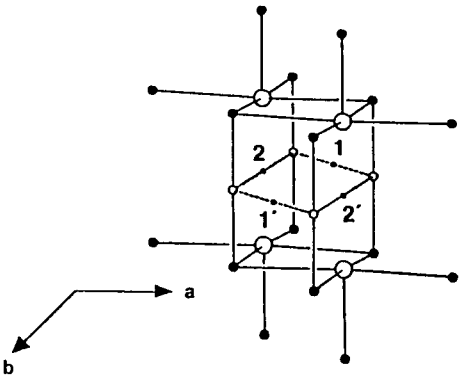


**Figure 5.** Schematic illustration of the oxygen incorporation in the Cu layer of the crystal. The Pb and the Cu atoms are represented by large and small open circles, respectively. The oxygen atoms are represented by filled circles. The sites to be occupied by additional oxygen atoms are shown as smaller filled circles, labelled 1 and 2 (equivalent to 1′ and 2′).

midpoints of the lines connecting two Pb atoms of two PbO layers to make the Pb cations six-coordinated. When this is done, new Cu-O chains along the **b** axis formed in the $CuO_8$ layer make so long Cu-$O_{ad}$ bonds that the oxidation states of Cu atoms in the chain remain unchanged, while those of six-coordinated Pb atoms change from +2 to +4 as will be discussed later.

By analogy with the $YBa_2Cu_3O_{7-y}$ phase, $O_{ad}$ atoms may be assumed to go into the Cu layer of the $Pb_2CuO_4$ slab to form Cu-O bonds along the **a**+**b** axis of Figure 1 (see also the site 1 in Figure 5) and along the **b** axis of Figure 1 (see also the site 2 in Figure 5). We shall consider the effects of these additional oxygen atoms on the electronic structure, especially the formal oxidation states of Pb and Cu, and hence on the amount of holes on the $CuO_2$ layer. If site 2 is occupied by an additional oxygen, the formation of very short Pb-$O_{ad}$ (=1.762 Å) bonds and very long Cu-$O_{ad}$ (=2.732 Å) bonds is obtained. Occupation of site 1 by Oad produces the Cu-$O_{ad}$ and Cu-$O_{eq}$ bonds with distances of 1.927 and 1.830 Å, respectively, and long Pb-$O_{ad}$ (=2.611 Å) distances. Therefore, if the corner-sharing square $CuO_3$ chains were to be formed along the **a**+**b** direction, the Cu coordinate environment of these chains will be similar to that found in the $YBa_2Cu_3O_{7-y}$.[10] One would expect $Pb_2Sr_2Y_{1-x}Ca_xCu_3O_9$ as the resulting product, but the existence of such ordering is not yet known.

The incorporation of an $O_{ad}$ atom into site 1 of unit cell corresponding to the addition of 0.5 O per unit formula as the first step of the oxidation process does not raise the Pb 6s-block and the Cu 3d-block bands above the Fermi level (refer to Figure 6). This means that an oxygen incorporation into this site (**5**→**6**) does not alter the formal oxidation states of $Pb^{2+}$ and $Cu^+$. In this case two electrons the $O_{ad}$ atom gains to form $O_{ad}^{2-}$ should come from the $CuO_2$ layer, which results in hole creation in the layer. This is true only when the four-coordinate Cu sites are not formed by $O_{ad}$. If the chain grows along the **a**+**b** direction as shown in the process **6**→**7**, the four-coordinate copper sites would be formed. For the same geometry as in the solid such

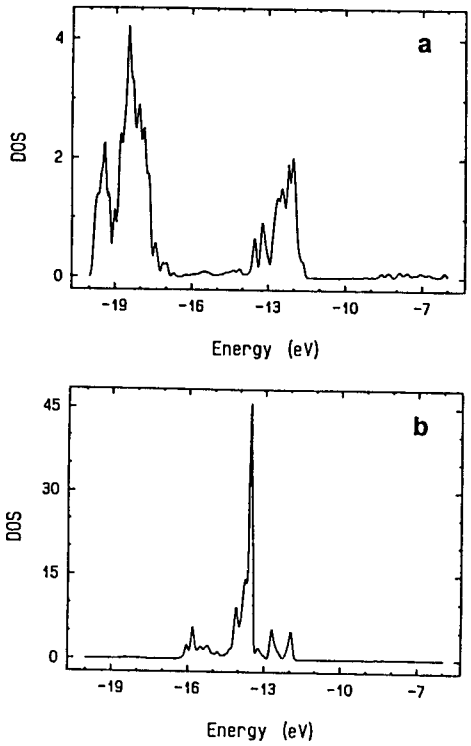


**Figure 6.** Projected DOS plots on Pb 6s (a) and Cu 3d (b) in $Pb_2CuO_{4.5}$ slab resulting from the incorporation of one $O_{ad}$ atom into site 1 of unit cell.

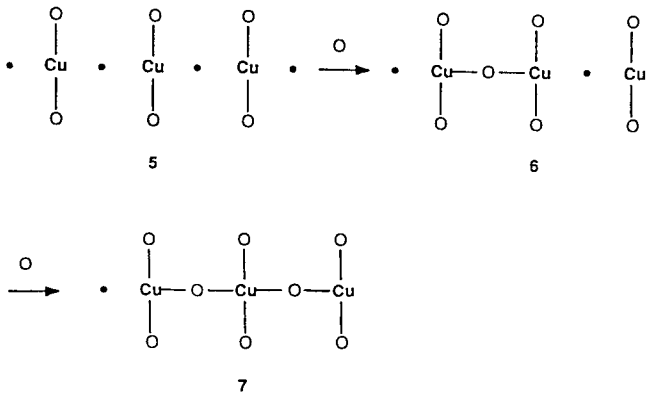


four-coordinate sites are very similar to those found in the $CuO_3$ chain of $YBa_2Cu_3O_{7-y}$[10] (Cu-O=1.830 and 1.927 Å for the former structure; Cu-O=1.850 and 1.943 Å for the latter). Therefore, the Cu oxidation state is expected to be +3 as in the $CuO_3$ chain of $YBa_2Cu_3O_{7-y}$. In Figure 7 we see the DOS curves calculated for the $Pb_2CuO_5$ slab containing the coordination environment of such copper atoms. The Pb 6s peaks lie below the Fermi level, so that the Pb oxidation state is +2. The presence of a peak corresponding to the highest-lying Cu $x^2$-$y^2$ band just above the Fermi level confirms the presence of $Cu^{3+}$ in $d^8$ state. The **5**→**6** gives rise to the creation of holes in the $CuO_2$ layers, but the **6**→**7** does not change the hole concentration of the layer because a second $O_{ad}$ atom traps two electrons released by a change of the four-coordinate copper oxidation state from +1 to +3. The incorporation of an $O_{ad}$ atom into site 2 as the second step of the oxidation process raises the Pb 6s-block

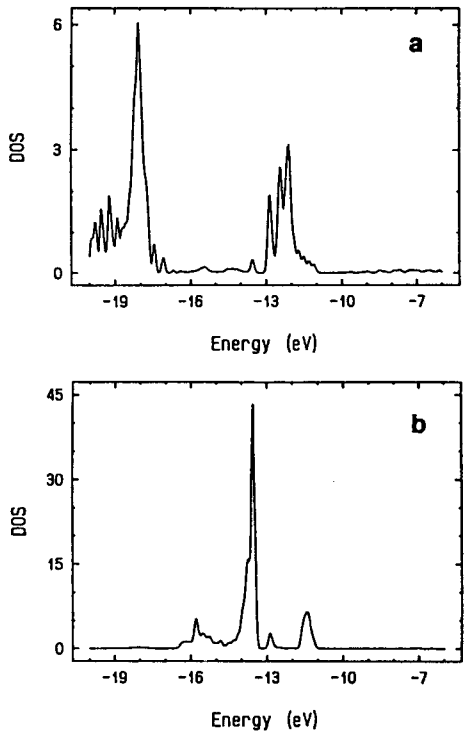


**Figure 7.** Projected DOS plots on Pb 6s (a) and Cu 3d (b) in $Pb_2CuO_5$ slab with the corner-sharing square $CuO_3$ chains along the **a**+**b** axis.

bands well above the Fermi level so that they are lying around −9.5 eV as shown in the DOS and COOP curves of Figures 8a and b. However, the Cu 3d-block bands are not shifted to higher energies so that they still lie below the Fermi level as shown in the DOS curves of Figure 8c. The former situation happens because of the strong antibonding interactions of $O_{ad}$ 2p orbitals with Pb lone pair orbitals pointing toward the oxygen vacant site (*i.e.*, $O_{ad}$ site). Thus the most likely oxidation states of Pb and Cu are +4 and +1, respectively. This oxidation process in $Pb_2CuO_4$ slab is given by the following reactions:

$$2Pb^{2+} \rightarrow 2Pb^{4+} + 4e^- \text{ and}$$

$$O_{ad} + 2e^- \rightarrow O_{ad}^{2-}$$

Thus two extra electrons generated in this step are expected to remove holes in the $CuO_2$ layer. When δ increases beyond 0.5, this charge transfer leading to underdoped hole region is responsible for the suppression of superconductivity due to the decrease of the hole concentration in the $CuO_2$ layers in $Pb_2Sr_2Y_{1-x}Ca_xCu_3O_{8+\delta}$, which is in good agreement with the increase in resistivity and Hall coefficient with increasing δ.[4]

The experimental observations[4] for the occurrence of *c*-axis expansion near $\delta = 1.0$ and the dependence on δ of the average oxidation states of Pb and Cu in $Pb_2Sr_2Y_{1-x}Ca_xCu_3O_{8+\delta}$ indicate that the oxidation of $Pb^{2+}$ to $Pb^{4+}$ should take place after $Cu^+$ oxidizes to $Cu^{3+}$. The latter observation has shown that the average oxidation state of Cu increases with increasing δ up to $\delta = 0.5$ and almost constant for $0.5 < \delta < 1.8$, while that of Pb increases with increasing δ for $0.5 < \delta < 1.8$. Since the Pb-$O_{ad}$ bond distance (1.762 Å) for $O_{ad}$ at the site 2 is extremely short, the expansion of the *c*-axis due to the increase in this bond is expected for oxygen incorporation

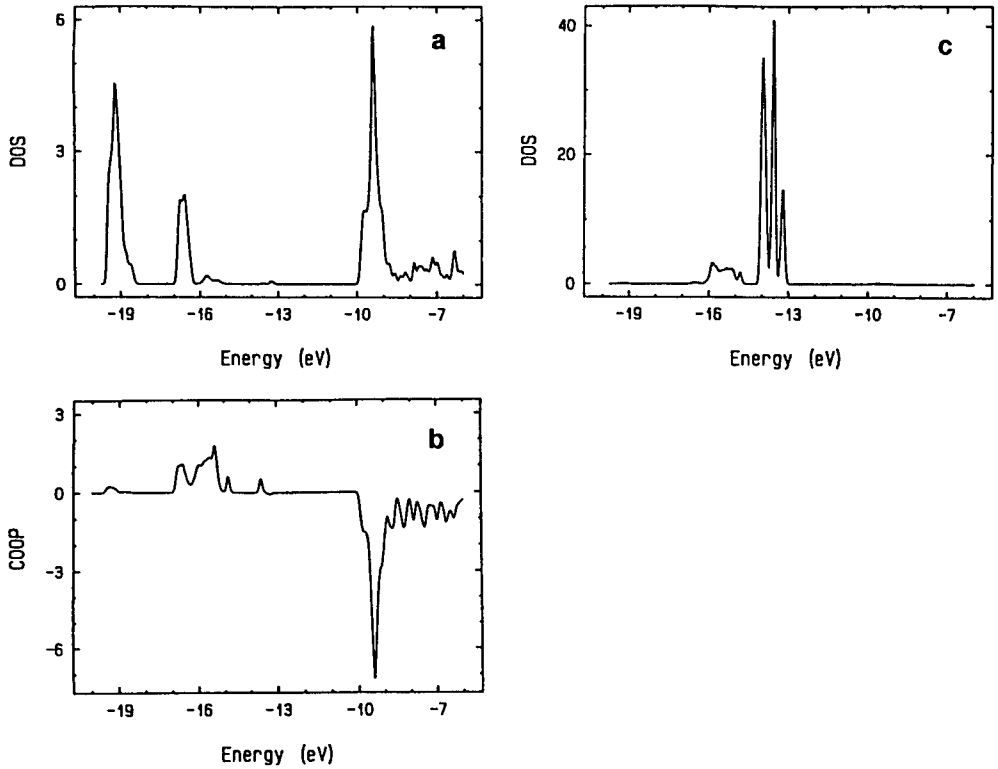


**Figure 8.** Projected DOS plots on Pb 6s (a) and Cu 3d (c) and COOP plots for the Pb-O bonds (b) in $Pb_2CuO_5$ slab resulting from the incorporation of two $O_{ad}$ atoms into sites 2 and 2′ of unit cell.

in the site. These results strongly corroborate the above oxidation process that at the beginning of oxidation $Cu^+$ oxidizes to $Cu^{3+}$ by forming corner-sharing square chains without oxidation of $Pb^{2+}$ to $Pb^{4+}$, and after a certain amount of oxygen incorporation $Pb^{2+}$ oxidizes to $Pb^{4+}$ by accommodating oxygen further at site 2 without any change of copper oxidation states. It is worthwhile to point out that the oxidation process of $Pb_2Sr_2Y_{1-x}Ca_xCu_3O_8$ takes place by layers while that of $YBa_2Cu_3O_6$ takes place by chains.

If the Cu-$O_{eq}$ distance is increased by the *c*-axis expansion occurring during the additional oxygen incorporation, the highest-lying 3d-block band of the four-coordinate copper will be lowered due to the decrease in Cu-O antibonding, thereby making the site good for $Cu^{2+}$, which is consistent with the observation of $Cu^{2+}$.[1] One can also consider the chain formation along the **b** axis. In this case, however, the Cu-$O_{ad}$ distance (2.732 Å) of the resulting four-coordinate site is so long that the site is most likely to be in the oxidation state of $Cu^+$ rather than $Cu^{3+}$.

## Conclusions

We have explored the formal oxidation states of Pb and Cu in the $Pb_2CuO_4$ slab of $Pb_2Sr_2Y_{1-x}Ca_xCu_3O_8$ and their possible changes by oxygen incorporation in the Cu layer within the slab. We find that they play a crucial role for the copper oxidation state of the $CuO_2$ layer which depends on the hole concentration of the layer. The oxidation states of Pb and Cu atoms in the $Pb_2CuO_4$ slab are +2 and +1, respectively. When the additional oxygen is incorporated in the Cu layer of the $Pb_2CuO_4$ slab, the corner-sharing square chains are formed first along the **a**+**b** axis, and then after the formation of these chain fragments, further oxidation takes place at the site 2 (see Figure 5) to give short Pb-$O_{ad}$ distances. For the four-coordinate Cu atoms in the square chains the formal oxidation state of +3 is assigned. The decrease of $T_c$ during the formation of chain fragments can be explained in terms of over-doping due to hole creation in the $CuO_2$ layer and the suppression of superconductivity by further oxygen incorporation in the site 2 along the **b** axis can be attributed to the decrease of holes in the $CuO_2$ layer caused by a change of the Pb oxidation state from +2 to +4.

**Acknowledgment.** This work was supported in part by a grant from the Kyungsung University Research Fund, 1994.

## References

1. Cava, R. J.; Baltlogg, B.; Krajewski, J. J.; Rupp, L. W.; Schneemeyer, L. F.; Siegrist, T.; VanDover, R. B.; Marsh, P.; Peck, W. F. Jr.; Gallagher, P. K.; Glarum, S. H.; Marshall, J. H.; Farrow, R. C.; Waszczak, J. V.; Hull, R.; Trevor, P. *Nature* **1988**, *336*, 211.
2. Subramanian, M. A.; Gopalakrishnan, J.; Torardi, C. C.; Gai, P. L.; Boyes, E. D.; Askew, T. R.; Flippen, R. B.; Farneth, W. E.; Sleight, A. W. *Physica C* **1989**, *157*, 124.
3. Whangbo, M.-H.; Kang, D. B.; Torardi, C. C. *Physica C* **1989**, *158*, 371.
4. Koike, Y.; Sunagawa, H.; Noji, T.; Masuzawa, M.; Kobayashi, N.; Namiki, M.; Hirokawa, K.; Saito, Y. *Physica C* **1990**, *171*, 331.
5. Whangbo, M.-H.; Hoffmann, R. *J. Am. Chem. Soc.* **1978**, *100*, 6093.
6. Hoffmann, R. *J. Chem. Phys.* **1963**, *39*, 1397. A modified Wolfsberg-Helmholz formula was used to calculate the off-diagonal $H_{ij}$ values: Ammeter, J. H.; Bürgi, H.-B.; Thibeault, J.; Hoffmann, R. *J. Am. Chem. Soc.* **1978**, *100*, 3686.
7. Ren, J.; Jung, D.; Whangbo, M.-H.; Tarascon, J. M.; LePage, Y.; Torardi, C. C. *Physica C* **1989**, *158*, 501; **1989**, *159*, 151.
8. Jung, D.; Whangbo, M.-H.; Herron, N.; Torardi, C. C. *Physica C* **1989**, *160*, 381.
9. Koike, Y.; Masuzawa, M.; Noji, T.; Sunagawa, H.; Kawabe, H.; Kobayashi, N.; Saito, Y. *Physica C* **1990**, *170*, 130.
10. Beno, M. A.; Soderholm, L.; Capone II, D. W.; Hinks, D. G.; Jorgensen, J. D.; Schuller, I. K.; Segre, C. U.; Zhang, K.; Grace, J. D. *Appl. Phys. Lett.* **1987**, *51*, 57.